

Evaluation of gravel sphericity and roundness based on surface-area measurement with a laser scanner

Yuichi Hayakawa^{a,*} and Takashi Oguchi^b

^a *Department of Earth and Planetary Science, Graduate School of Science, The University of Tokyo, 7-3-1 Hongo, Bunkyo-ku, Tokyo 113-0033, Japan*

^b *Center for Spatial Information Science, The University of Tokyo, 4-6-1, Komaba, Meguro-ku, Tokyo 153-8904, Japan*

**E-mail address: hayakawa@csis.u-tokyo.ac.jp*

ABSTRACT

Sphericity and roundness have been employed in sedimentological and geomorphological studies to represent the gross shape of a gravel particle. The original complex definitions of gravel sphericity and roundness led to the use of visual charts or simplified parameters. Although the accurate derivation of sphericity requires the surface area of a gravel particle, manual measurement of the area is extremely difficult. To obtain the surface area and to calculate sphericity based on the original definition, 3D digital models of gravel particles were constructed using a laser scanner. The scanned gravel samples, collected from a riverbed in central Japan, include various shapes from angular to well-rounded. The obtained true sphericity values show an unexpectedly high correlation with Krumbein's roundness, despite that sphericity and roundness have been regarded as different concepts. Such a high correlation may reduce the value of one of the parameters. As a spherical particle of gravel rarely occurs in nature, a new parameter, a modification of the true sphericity, is proposed to express the deviation of gravel shape from an ellipsoid with given axis lengths. The parameter has a very weak correlation with roundness and gravel size, suggesting its independence and potential usefulness. The surface area data also permit the estimation of gravel roundness without using a visual chart.

Keywords: shape index, three dimensional scanning, geometric surface model, ellipsoid, correlation analysis

1. Introduction

The size and shape of gravel particles on earth surfaces or in deposits have been analyzed since long time ago, to better understand the processes of fluvial and eolian transport (Stokes, 1851; Hjulstrom, 1935; Bagnold, 1941; Inman, 1949; Gibbs et al., 1971; Miller et al., 1977; Baba and Komar, 1981; Pye, 1994; Le Roux, 1996) and to discuss the past environmental conditions such as paleoflood depth (Baker, 1974; Komar 1989; Evans, 1991; Howard, 1992; O'Connor, 1993; Sugai, 1993; Plakht, 1998; Grossman, 2001; Jacobson et al., 2003). The most frequently used and easy-to-measure gravel-size parameters are the lengths of the three representative axes: a (major/maximum axis length), b (medium axis length) and c (minor axis length). These lengths are equivalent to the side lengths of a rectangular-solid box bounding a particle. The medium axis length (b) has often been regarded as the most representative particle-size dimension (Griffiths, 1967). The volume of a gravel particle (V) can also be measured readily by immersion in a fluid. The nominal diameter (d_n), the diameter of a sphere having the same volume as V , has also been used as a representative gravel length (Lane et al., 1947; Komar and Reimers, 1978). Some gravel-shape parameters such as the elongation ratio (b/a , Koster and Leser, 1967) and the flatness ratio ($(a+b)/2c$, Wentworth, 1919; $c/(ab)^{1/2}$, Goguel, 1953) have been derived from the axis lengths. Some other indices derived from the three axis lengths correlate well with the settling velocity of gravel particles (Hoffman, 1994; LeRoux, 2004).

Besides these gravel lengths and their derivatives, two parameters expressing the entire shape of a gravel particle, sphericity and roundness, have received attention since a long time ago. Sphericity represents a gross gravel shape, whereas roundness represents the angularity of corners (Wadell, 1932, 1933). Roundness reflects the transportation processes, especially transported distance (Beal and Shepard, 1956; Kuenen, 1956; Shepard and Young, 1961).

However, the determination of gravel sphericity and roundness based on Wadell's original definitions is difficult. For instance, the surface area of a gravel particle is necessary to calculate Wadell's original sphericity, although its accurate manual measurement is almost impossible. Therefore, simplified parameters and visual charts have been constructed to measure sphericity and roundness (Wadell, 1933; Krumbein, 1941; Rittenhouse, 1943; Cailleux, 1952; Kuenen, 1956; Sneed and Folk, 1958).

This paper examines some hard-to-measure gravel-shape parameters such as Wadell's original sphericity, based on surface-area data acquired by a laser scanner. The recent development of laser scanners has enabled the construction of detailed surface geometric models in 2D or 3D. Although this technology, combined with remote sensing, has been employed to construct digital elevation models (e.g., Bornaz et al., 2002; Nagihara et al., 2004), laser scanners for measuring small objects in laboratories have not been widely used in earth science. This study presents an example of geoscientific applications of such scanners. We also propose new indices for objective and quantitative representation of the general shape of a gravel particle.

2. Previous studies on gravel sphericity and roundness

Sphericity (ψ) describes how closely a rock particle resembles a sphere. It was originally defined as s_n/S , where S is the surface area and s_n is the nominal surface area, i.e. the surface area of a sphere having the same volume as the particle (Wadell, 1932). Although Wadell (1932) called this index true sphericity, manual measurement of S is extremely difficult. Therefore Wadell (1933) proposed a simplified sphericity parameter, d_n/D , where D is the diameter of a minimum sphere

circumscribing a gravel particle. D has often been substituted for by a for faster calculation (Krumbein, 1941). Sphericity indices derived from axis lengths have also been proposed: $(bc/a^2)^{1/3}$ (Krumbein, 1941) and $(c^2/ab)^{1/3}$ (Sneed and Folk, 1958). These simplified indices are imperfect because an asteroid-like particle and an elliptic particle yield the same value if they have the same axis lengths. Therefore, Rittenhouse (1943) provided a visual chart for the practical determination of sphericity, but the evaluation of the true sphericity based on Wadell's original definition has yet to be performed.

Roundness (X_v) represents the curvature of particle's corners. Wentworth (1919) measured roundness using corners on the maximum projection plane that includes both the major and medium axes. Wadell (1933) thus defined roundness as $\sum (r_i/RN)$, where r_i is the radius of an inscribed circle for each corner of the gravel outline on the maximum projection plane, R is the radius of the maximum inscribed circle, and N is the number of corners. Simplified roundness indices using only the radius of the most curved corner as well as a and b have been proposed (Cailleux, 1952; Kuenen, 1956). However, objective identification of curved corners is difficult because the outline of a gravel particle includes various scales of curvature. At the smallest scale, a protruded mineral crystal may provide a highly curved corner, although it does not represent gravel roundness. Therefore, the applications of the above roundness parameters have been limited. Krumbein (1941) therefore provided a chart dividing visual roundness into ten classes. This chart and revised ones (Powers, 1953; Shepard and Young, 1961) have often been used for rapid field measurement. As mentioned by Wadell (1933), sphericity and roundness are different concepts, since the former represents the gross shape of a particle while the latter focuses on particle corners. Most roundness parameters so far proposed require shape projection onto a two-dimensional surface and manual selection of corners.

3. Acquisition of 3D gravel models

Fifty gravel samples were collected from a gravel bar in the middle reach of the Nakagawa River, Ibaraki Prefecture, Japan (N36°33'33", E140°14'58"). The catchment of the river is mostly underlain by Tertiary sedimentary and Quaternary volcanic rocks, and the samples comprise of welded tuff, chart, mudstone, sandstone, andesite and diolite. Frequent floods along the river (Jones et al., 2001) have transported abundant coarse sediment to downstream areas. The gravel samples encompass various shapes from angular to well-rounded, with maximum lengths between 6 and 12 cm.

The three-dimensional scanner used is the LPX-250, Roland DG Corporation (approximate price is \$13,500, as of December 2004). This box style scanner has a rotating table at the inner bottom on which a target object is placed. A spot laser beam (wavelength: 660-700 nm, frequency: 2,857 Hz) is emitted from a movable unit onto the object. The unit also has a sensor to catch the light reflected from the object. The sensor signals are converted into point data with three-dimensional spatial coordinates. The maximum size of the scannable object is 254 mm in diameter and 406.4 mm in height. The scanner has two operation modes: 1) rotary scanning in which the laser beam emitted from the vertically moving unit travels onto the rotating object to scan the whole surface; and 2) plane scanning in which an aspect of the object is scanned in one operation using parallel laser beams while the table and laser unit rotates in synchronization. The rotary mode was applied in this study since it is suitable for sphere- or cylinder-like objects such as particles of fluvial gravel. The possible minimum pitch of the rotary scanning is 0.2 degrees in circumference and 0.2 mm in height. We operationally applied a pitch of 1.0 degree in circumference and 0.4 mm in height to obtain detailed data while limiting file sizes: 1.4 to 4.4 MB for each sample. Before

scanning, the gravel samples were washed with water to remove sand and mud. Then each gravel particle was placed on a rubber pedestal on the rotation table of the scanner. Since the laser beam is horizontal, the top and bottom of a gravel sample cannot be scanned precisely. To obtain accurate data, we performed scanning twice for each particle of gravel with different sample orientations at nearly right angles.

The obtained geometric data of gravel surfaces were edited using PixForm 1.0, a Windows-based software package from Roland DG Corporation (Fig. 1). First, the scanned pedestal and adjacent low-quality data for the lowermost part of a gravel sample were deleted. Then, the two models with different orientations were aligned and merged using the default function of the software. Obvious noise and small holes on the merged model, originated from improper reflection of the laser due to local surface conditions such as colors of minerals, were corrected using a spatial interpolation function. Because data for nine samples had some large holes, we analyzed the data only for the remaining 41 samples. The spatial distribution of the data points was optimized using an interpolation module in PixForm. Fig. 2 shows that the irregular frequency distribution of triangular face areas was corrected through the optimization. The standard deviation of the face area also decreased from 0.100 mm^2 to 0.073 mm^2 . Although it took about twenty minutes to complete one scanning operation, the post-processing of the scanned data took much more time, depending on the degree of data complexity and the capacity of the personal computer used.

4. Derivation of true sphericity and relevant gravel shape parameters

The constructed 3D geometric models permit objective evaluation of sphericity including that based on the original

definition. The volume (V) and surface area (S) of a particle of gravel can be readily obtained from the models. The nominal diameter (d_n) and nominal surface area (s_n) can be calculated from V : $d_n = (6V/\pi)^{1/3}$ and $s_n = (36\pi V^2)^{1/3}$. Accurate values for a , b and c are also available because the three gravel axes can be automatically determined. From these parameters, we computed Wadell's (1932) true sphericity (s_n/S) and three alternative sphericity indices: d_n/a , $(bc/a^2)^{1/3}$ and $(c^2/ab)^{1/3}$.

We also propose a new index of general gravel shapes by modifying Wadell's sphericity. Although sphericity indicates how much a particle of gravel resembles a sphere, ball-like rock particles are rarely found in natural deposits. Thus, not a sphere but an ellipsoid can be regarded as an ideal gravel form. To express the similarity of a gravel particle to an ellipsoid with the same axis lengths, a parameter E_s is defined as e_n/S , where e_n is the surface area of an ellipsoid having axis lengths of a , b and c . The calculation of e_n is based on the elliptic integral:

$$e_n = \frac{\pi}{2} (c^2 + b\sqrt{a^2 - c^2} \int_0^\alpha \sqrt{1 - k^2 \sin^2 \varphi} d\varphi + \frac{bc^2}{\sqrt{a^2 - c^2}} \int_0^\alpha \frac{d\varphi}{\sqrt{1 - k^2 \sin^2 \varphi}}) \quad (1)$$

where $k^2 = (1 - c^2/b^2)/(1 - c^2/a^2)$, $\alpha = \sin^{-1}(1 - c^2/a^2)^{1/2}$, and φ is a temporal parameter for the integration. Since there is no explicit analytical solution for the integrals in the above equation, we performed numerical integration using the Simpson formula to derive e_n from the measured values of a , b and c . Then, the E_s index was computed for each gravel sample. We also visually determined roundness (X_v) using the chart of Krumbein (1941). In addition, three indices useful for predicting the settling velocity, H_r , $(1-c/b)^{0.5}$ and $(1-c/a)^{2.5}$ (Hoffman, 1994; LeRoux, 2004), were calculated using the lengths of the three major gravel axes.

5. Correlations between gravel shape parameters

Correlations between the obtained gravel-shape parameters were investigated (Table 1). Strong positive correlations between the parameters that directly reflect gravel sizes (a , b , c , V , S , d_n , s_n and e_n) shown in the upper left of Table 1 are self-evident. Thus, attention is paid to the other correlations.

Table 1 suggests that the previously proposed sphericity parameters are of limited use. Although sphericity needs to be independent of roundness according to their definitions, Wadell's true sphericity (s_n/S) shows an unexpectedly high correlation with Krumbein's roundness (Table 1, Fig. 3). The alternative sphericity indices (d_n/a , $(bc/a^2)^{1/3}$ and $(c^2/ab)^{1/3}$) have strong correlations with a and/or c , and such dependence on the size parameters is inappropriate for gravel-shape indices. The same applies to the indices related to the settling velocity of gravel particles, H_r , $(1-c/b)^{0.5}$ and $(1-c/a)^{2.5}$, because they are strongly correlated with c .

The E_s index ($= e_n/S$) seems to be more useful than sphericity as a measure of general gravel particle forms. Other than the similarity of ellipsoids to natural particles of gravel, the index is independent of roundness and gravel size because it poorly correlates with Krumbein's roundness and the length of the three axes (Table 1).

Wadell's true sphericity (s_n/S) may be used as a quantitative index of roundness because it correlates with Krumbein's roundness. The true sphericity can be regarded as a dimensionless ratio of V to S , since s_n is derived directly from V . For the same value of V , S tends to increase with increasing surface irregularity or angularity. Thus, the good correlation between the true sphericity and roundness is reasonable. However, the plot of the true sphericity and roundness shows relatively large scatter (Fig. 3).

We developed an improved roundness parameter based on the above idea that the volume/area ratio reflects roundness. The V/S ratio tends to increase with an increasing gravel size because it has a dimension of length. To remove the size effect, the ratio needs to be divided by a representative gravel length. In the case of Wadell's sphericity, the representative gravel length is equivalent to the nominal diameter (d_n). As an ellipsoid is a better analogue of gravel shape than a sphere, not a single diameter, but the lengths of all three axes seem to be important in evaluating the gravel length. Therefore, we adopted the geometric mean of a , b and c as a representative gravel length. The resultant index $X_s = V/S(abc)^{1/3}$ shows a very strong correlation with Krumbein's roundness ($r^2 = 0.814$; Fig. 4), suggesting that the index can be used as an objective parameter of roundness. We also applied the arithmetic mean of a , b and c instead of the geometric mean, but it resulted in a weaker correlation ($r^2 = 0.707$).

6. Conclusions

The digital modeling of gravel particles based on 3D laser scanning has enabled accurate quantitative measurements of their shapes. Especially, the measurement of the surface area, which was practically impossible by manual methods, has provided an opportunity to reevaluate the previously proposed gravel shape parameters such as Wadell's original sphericity. Since we found that some existing indices are of limited use in describing the general shape of gravel particles, we have proposed new gravel-shape parameters: similarity to the ellipsoid with the same axis lengths (E_s) and a 3D roundness index (X_s).

Although E_s seems to give a solution to the problem with Wadell's original sphericity, i.e., strong correlations with roundness, its environmental implications remain to be examined. To address the issue, E_s needs to be measured for gravel samples from

various environmental conditions. This is left for future research.

The obtained 3D gravel models with numerous point data permit not only the evaluation of gross gravel shapes but also detailed investigation of small-scale surface texture. Such analyses are also left for future work. Currently the construction of 3D gravel models remains time-consuming. However, the future improvement in scanning devices and computer technology will lead to faster objective analysis of gravel shapes in 3D. Then it will be possible to test the validity of various gravel-shape parameters including those proposed in this study based on statistical treatments of a large amount of data.

ACKNOWLEDGEMENTS

We thank Dr. Michael Grossman for reading and commenting on an early draft.

REFERENCES CITED

- Baba, J., Komar, P.D., 1981. Measurements and analysis of settling velocities of natural quartz sand grains. *Journal of Sedimentary Petrology* 51, 631-640.
- Bagnold, R.A., 1941. *The Physics of Blown Sand and Desert Dunes*: London, Methuen.
- Baker, V.R., 1974. Paleohydraulic interpretation of quaternary alluvium near Golden, Colorado. *Quaternary Research* 4, 94-112.
- Beal, M.A., Shepard, F.P., 1956. A use of roundness for determining depositional environments. *Journal of Sedimentary Petrology* 26 (1), 49-60.
- Bornaz, L., Lingua, A., Rinaudo, F., 2002. Engineering and environmental applications of laser scanner techniques. *Proceedings of the International Archives of the Photogrammetry, Remote Sensing and Spatial Information Sciences* 34 (3B), pp. 40-43.
- Cailleux, A., 1952. Morphoskopische Analyse der Geschiebe und Sandkornen und ihre Bedeutung für die Palaoklimatologie. *Geologische Rundschau* 40, 11-19.
- Evans, D.J.A., 1991. A gravel/diamicton lag on the south Albertan prairies, Canada: evidence of bed armoring in deglacial

- sheet-flood/spillway courses. *Geological Society of America Bulletin* 103, 975-982.
- Gibbs, R.J., Matthews, M.D., Link, D.A., 1971. Relationship between sphere size and settling velocity. *Journal of Sedimentary Petrology* 41 (1), 7-18
- Goguel, J., 1953. A propos de la mesure des galetss et de la definition des indices. *Revue de Geomorphologie Dynamique* 4 (3), 115-118.
- Griffiths, J.C., 1967. *Scientific Method in Analysis of Sediments*. McGraw-Hill, New York, 508 pp.
- Grossman, M.J., 2001. Large floods and climatic change during the Holocene on the Ara River, Central Japan. *Geomorphology* 39, 21-37.
- Hjulström, F., 1935. Studies of the morphological activity of rivers as illustrated by the river Fyris. *Bulletin of Geological Institute of Uppsala* 25, 221-527.
- Hoffman, H.J., 1994. Grain-shape indices and isometric graphs. *Journal of Sedimentary Research* A64, 916-920.
- Howard, J.L., 1992. An evaluation of shape indices as paleoenvironmental indicators using quartzite and metavolcanic clasts in Upper Cretaceous to Palaeogene beach, river and submarine fan conglomerates. *Sedimentology* 39, 471-468.
- Inman, D.L., 1949. Sorting of sediments in the light of fluid mechanics. *Journal of Sedimentology and Petrology* 19, 51–70.
- Jacobson, R.B., O'Conner, J.E., Oguchi, T., 2003. Surficial geologic tools in fluvial geomorphology. In: Kondolf, G.M., Piegay, H., (Eds.), *Tools in Fluvial Geomorphology*. John Wiley and Sons, New York, pp. 25-57.
- Jones, AP, Shimazu, H., Oguchi, T., Okuno, M., Tokutake, M., 2001. Late Holocene slackwater deposits on the Nakagawa River, Tochigi Prefecture, Japan. *Geomorphology* 39, 39-51.

- Komar, P.D., Reimers, C.E., 1978. Grain shape effects on settling rates. *Journal of Geology* 86, 193-209.
- Komar, P.D., 1989. Flow-competence evaluations of the hydraulic parameters of floods: an assessment of the technique. In: Beven, K., Carling, P., (Eds.), *Floods: hydrological, sedimentological and geomorphological implications*. John Wiley and Sons, Chichester, pp. 107-134.
- Köster, E., Leser, H., 1967. *Geomorphologie I. Bodenkundliche Methoden, Morphometrie und Granulometrie*. Westermann, Braunschweig, 131 pp.
- Krumbein, W.C., 1941. Measurement and geological significance of shape and roundness of sedimentary particles. *Journal of Sedimentary Petrology* 11, 64-72.
- Kuenen, Ph.H., 1956. Experimental abrasion of pebbles: 2. Rolling by currents. *Journal of Geology* 64, 336-368.
- Lane, E.W., 1947. Report of the subcommittee on sediment terminology. *Transactions, American Geophysical Union* 28, 936-938.
- Le Roux, J.P., 1996, Settling velocity of ellipsoidal grains as related to shape entropy. *Sedimentary Geology* 101, 15-20.
- Le Roux, J.P., 2004, A hydrodynamic classification of grain shapes. *Journal of Sedimentary Research* 74, 135-143.
- Miller, M.C., McCave, I.N., Komar, P.D., 1977. Threshold of sediment motion under unidirectional currents. *Sedimentology* 24, 507-527.
- Nagihara, S., Mulligan, K.R., Xiong, W., 2004. Use of a three-dimensional laser scanner to digitally capture the topography of sand dunes in high spatial resolution. *Earth Surface Processes and Landforms* 29, 391-398.
- O'Connor, J.E., 1993. Hydrology, hydraulics and geomorphology of the Bonneville flood. *Special Paper 274, Geological*

- Society of America. Boulder, Colorado, 83 pp.
- Plakht, J., 1998. Shape of pebbles as an indicator of climatic changes during the Quaternary in Makhtesh Ramon, Negev, Israel. *Zeitschrift für Geomorphologie Neue Folge* 42, 221-231.
- Powers, M.C., 1953. A new roundness scale for sedimentary particles. *Journal of Sedimentary Petrology* 23, 117-119.
- Pye, K., ed., 1994. *Sediment Transport and Depositional Processes*. Blackwell Scientific Publications, Oxford, 397 pp.
- Shepard, F.P., Young, R., 1961. Distinguishing between beach and dune sands. *Journal of Sedimentary Petrology* 31, 196-214.
- Sneed, E.D., Folk, R.L., 1958. Pebbles in the lower Colorado river, Texas: A study in particle morphogenesis. *Journal of Geology* 66, 114-150.
- Stokes, G.G., 1851. On the effect of the internal friction of fluids on the motion of pendulums. *Transactions of the Cambridge Philosophical Society* 9 (2), 8-106.
- Sugai, T., 1993. River terrace development by concurrent fluvial processes and climate change. *Geomorphology* 6, 243-252.
- Wadell, H., 1932. Volume, shape, and roundness of rock particles. *Journal of Geology* 40, 443-451.
- Wadell, H., 1933. Sphericity and roundness of rock particles. *Journal of Geology* 41, 310-331.
- Wadell, H., 1935. Volume, shape and roundness of quartz particles. *Journal of Geology* 43, 250-280.
- Wentworth, C.K., 1919. A laboratory and field study of cobble abrasion. *Journal of Geology* 27, 507-521.
- Zingg, T., 1935. Beitrag zur Schotteranalyse. *Schweizer Mineralogie und Petermanns Mitteilungen* 15, 39-140.

Figure captions

Fig. 1. Procedure for gravel model construction.

Fig. 2. Histograms of face areas in 3D model of gravel piece No. 1. A: Original. B: After re-organization.

Fig. 3. Relationship between Wadell's sphericity (s_n/S) and Krumbein's roundness (X_v).

Fig. 4. Relationship between new roundness index (X_s) and Krumbein's roundness (X_v).

Fig. 1.

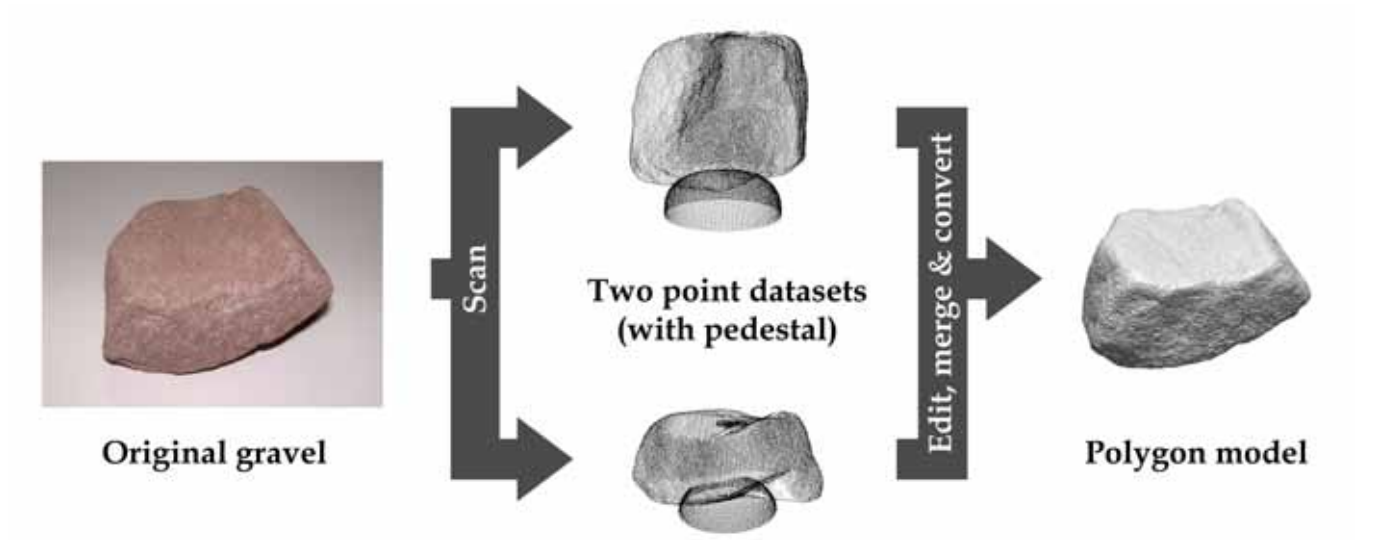


Fig. 2.

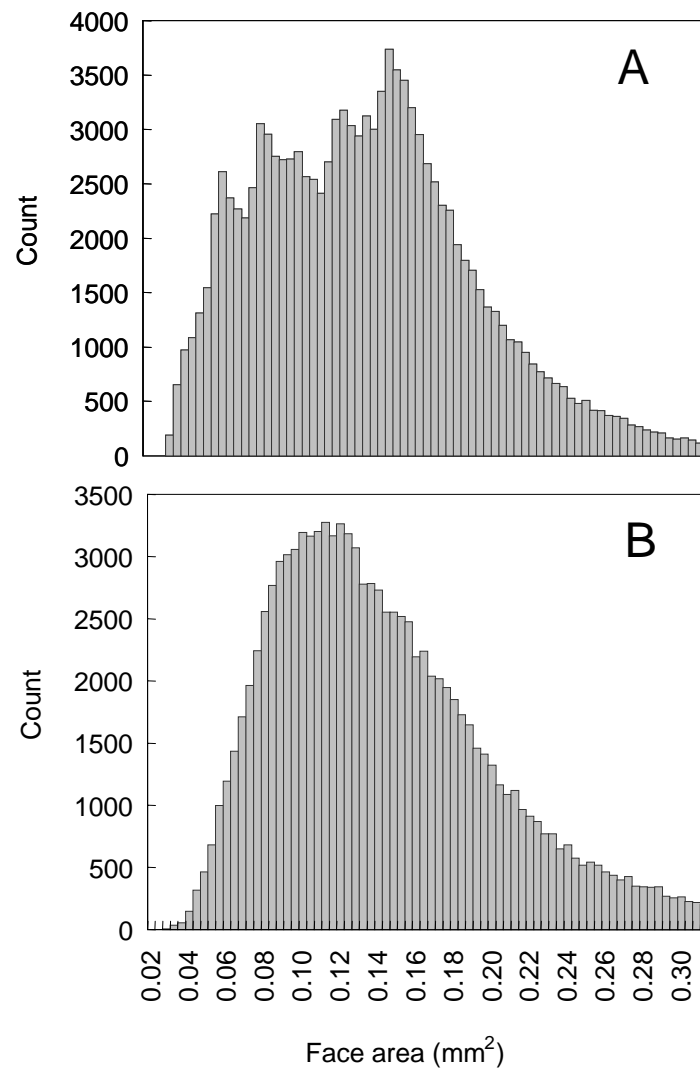
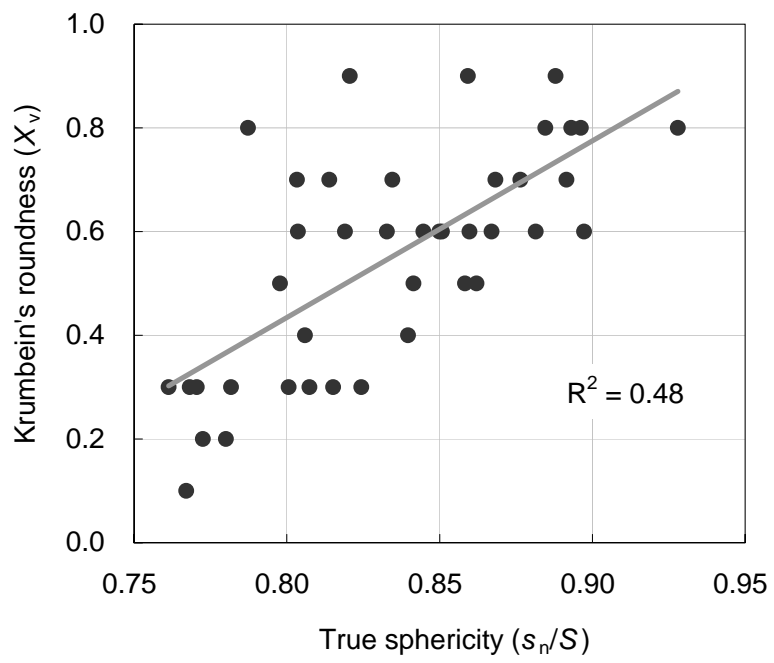


Fig. 3.



Tables

Table 1. Correlation coefficients between shape indices.

	<i>a</i>	<i>b</i>	<i>c</i>	<i>V</i>	<i>S</i>	<i>d_n</i>	<i>s_n</i>	<i>e_n</i>	Sphericity indices			Settling-velocity predicting indices								
									<i>s_n/S</i>	<i>d_n/a</i>	$(bc/a^2)^{1/3}(c^2/ab)^{1/3}$	<i>H_t</i>	$(1-c/b)^{0.5}$	$(1-c/a)^{2.5}$	<i>E_s</i>	<i>X_v</i>	<i>X_s</i>			
<i>a</i>		+++	++	+++	+++	+++	+++	+++												
<i>b</i>	0.544		++	+++	+++	+++	+++	+++												
<i>c</i>	0.414	0.456		+++	+++	+++	+++	+++												
<i>V</i>	0.795	0.713	0.784		+++	+++	+++	+++												
<i>S</i>	0.847	0.770	0.744	0.964		+++	+++	+++												
<i>d_n</i>	0.805	0.746	0.792	0.987	0.976		+++	+++												
<i>s_n</i>	0.802	0.732	0.791	0.997	0.973	0.997		+++												
<i>e_n</i>	0.819	0.787	0.791	0.965	0.979	0.972	0.972													
<i>s_n/S</i>	-0.240	-0.224	0.200	0.087	-0.158	0.044	0.066	-0.072												
<i>d_n/a</i>	-0.503	0.156	0.448	0.096	-0.004	0.101	0.099	0.031	0.471											
$(bc/a^2)^{1/3}$	-0.379	0.283	0.617	0.190	0.135	0.206	0.199	0.201	0.303	0.931										
$(c^2/ab)^{1/3}$	-0.044	0.005	0.849	0.383	0.308	0.388	0.387	0.361	0.388	0.640	0.747									
<i>H_t</i>	-0.159	0.157	0.799	0.342	0.275	0.358	0.351	0.333	0.368	0.777	0.887	0.931								
$(1-c/b)^{0.5}$	-0.042	0.157	-0.782	-0.364	-0.286	-0.356	-0.361	-0.320	-0.371	-0.456	-0.532	-0.944	-0.777							
$(1-c/a)^{2.5}$	0.184	-0.141	-0.797	-0.326	-0.260	-0.339	-0.334	-0.317	-0.359	-0.796	-0.903	-0.941	-0.995	0.794						
<i>E_s</i>	0.013	0.185	0.314	0.138	0.039	0.120	0.130	0.239	0.406	0.124	0.302	0.279	-0.110	-0.180	0.083					
<i>X_v</i>	-0.218	-0.228	-0.239	-0.098	-0.291	-0.153	-0.126	-0.263	0.689	0.160	-0.087	-0.132	-0.011	-0.294	0.167	0.088				+++
<i>X_s</i>	-0.264	-0.351	-0.133	-0.068	-0.295	-0.117	-0.093	-0.274	0.894	0.292	0.001	0.056	0.014	0.304	-0.185	0.063	0.814			

a: major axis length, *b*: medium axis length, *c*: minor axis length, *V*: volume, *S*: surface area, *d_n*: nominal diameter, *s_n*: nominal surface area, *e_n*: surface area of ellipsoid for given *a*, *b* and *c*, *H_t*: Hoffman's index, *E_s*: *e_n/S*, *X_v*: Krumbein's roundness, *X_s*: $V/(S(abc)^{1/3})$.

+++ : positive correlation with > 99% significance. ++ : positive correlation with 95-99% significance. + : positive correlation with 90-95% significance. --- : negative correlation with > 99% significance. -- : negative correlation with 95-99% significance. - : negative correlation with 90-95% significance.